Simplex splitting in the light actinides

M. W. Drigert* and J. A. Cizewski
A. W. Wright Nuclear Structure Laboratory, Yale University, New Haven, Connecticut 06511
(Received 24 December 1985)

The structure of the nucleus ^{219}Ac($Z=89, N=130$) has been studied via the ^{209}Bi(^{13}C,3n)^{219}Ac reaction. In-beam γ-ray spectroscopic techniques, including γ-ray and α-particle excitation functions, α-γ coincidence, γ-γ coincidence, and γ-ray angular distribution measurements were used in the construction of a level scheme up to a spin of $J=\frac{31}{2}\hbar$ at an excitation energy of 2245 keV. A total of five bands have been constructed and a series of parity doublets has been observed. For four of the bands the states have been labeled in terms of the simplex quantum number, which should be an appropriate quantum number even for octupole deformed nuclei. However, considerable simplex splitting is observed. The level scheme of ^{219}Ac indicates that the nucleus lies in the boundary region between the single-particle shell structure seen in the nuclei immediately surrounding ^{208}Pb and the collective rotational structure prevalent in the heavier actinides. However, no detailed model predictions are, as yet, available to describe the observed structure, which may require quadrupole, octupole, and nonaxial degrees of freedom.

I. INTRODUCTION

The study[1-16] of nuclei in the region beyond the doubly-magic nucleus ^{208}Pb has been of interest because this region affords an opportunity to investigate the interplay between single-particle and collective structures in nuclei as the number of valence nucleons outside of the doubly-magic core is varied and as angular momentum is added to the nuclear system. These studies have been aided by the appearance of high-spin yrast isomers which simplify the determination of the single-particle configurations.[1,2,11] The interest in this mass region has intensified with the introduction in the last few years of the alpha-particle cluster (vibron) model[17] and the stable octupole deformation model.[18,19] The vibron model has been utilized in describing the structure of ^{218}Ra (Ref. 4) and ^{220}Th (Ref. 16). The stable octupole deformation model has been used to explain some features of the heavier actinides,[19-24] in particular, the observation of parity doublets in these nuclei. The study of ^{219}Ac affords an opportunity to test the predictive abilities of these two models against the experimentally observed structures. At the start of this study the only information available on ^{219}Ac was its ground state α-decay energy and a proposed ground state spin.[25] Our preliminary results have been reported,[12-14] as have those of a concurrent study of ^{219}Ac in which similar experimental techniques[15] were used.

II. EXPERIMENTAL INSTRUMENTATION AND DATA ANALYSIS

The nucleus ^{219}Ac was populated via a ^{209}Bi(^{13}C,3n)^{219}Ac reaction with beams from the Yale MP tandem van de Graaff accelerator. The electromagnetic deexcitation of ^{219}Ac was studied using standard γ-ray spectroscopic techniques. The γ-ray detectors used for this investigation include an n-type high-purity, "gamma-X," Ge detector with a quoted efficiency [relative to a 7.6 cm$\times$7.6 cm NaI(Tl) scintillator] of 25% and three Ge(Li) detectors with efficiencies of 20%, 12%, and 5%, respectively. Typical energy resolutions measured for the four detectors were 2.11, 2.18, 2.45, and 2.37 keV FWHM, respectively, at 1332 keV.

An excitation function measurement was performed, over a range of ^{13}C beam energies from 60 to 73 MeV, on a ^{209}Bi target with an areal density of ≈ 1.0 mg/cm^2, collecting both γ-ray and α-particle data. The α particles were detected in a large area (450 mm^2) 300-μm thick Si surface-barrier detector with an energy resolution measured with a ^{228}Th α source to be 150 keV.

The peak of the ^{219}Ac production cross section was determined by the yield of α particles from the characteristic α-decay chain involving ^{219}Ac shown in Fig. 1. In Fig. 2 the α-particle spectra collected at ^{13}C beam energies

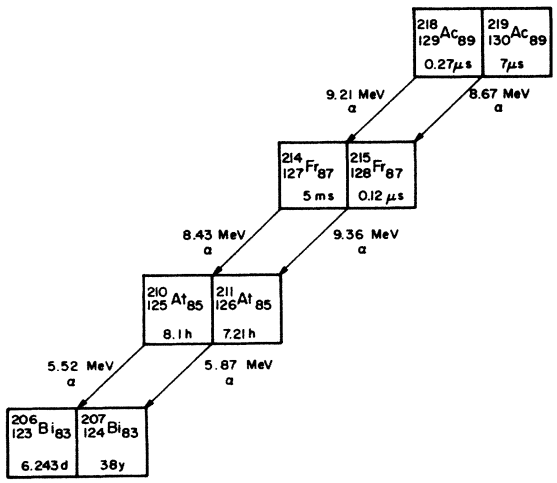

FIG. 1. Alpha-particle decay chain for ^{218}Ac and ^{219}Ac. The ground-state lifetimes and α-particle energies are indicated (Ref. 25).

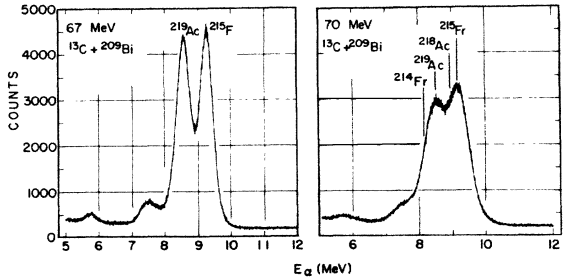

FIG. 2. Alpha-particle singles spectra taken at ^{13}C beam energies of 67 and 70 MeV. Alpha-particle energies associated with ground-state decay of ^{214}Fr, ^{215}Fr, ^{218}Ac, and ^{219}Ac are indicated (Ref. 25).

of 67 and 70 MeV are presented. At 67 MeV the ^{219}Ac and ^{215}Fr ($t_{1/2}=120$ ns) ground state α-decay transitions are clearly distinguished, with no evidence of competition from the ^{218}Ac 4n-reaction channel (see Fig. 1 for the α-particle energies). The situation changes drastically at a beam energy of 70 MeV where the ^{218}Ac production channel strongly competes with that of ^{219}Ac.

To determine which γ rays observed in the excitation function measurement originate from ^{219}Ac, a delayed α-γ coincidence measurement was performed. In Fig. 3 we present the γ-ray spectrum obtained in coincidence with the ^{219}Ac α-decay line. All of the strong γ-ray transitions between 130 and 450 keV have been placed in the ^{219}Ac level scheme. Because of the long decay time of the ground state of ^{219}Ac (≈ 7 μs) the γ-ray time signals were delayed 12 μs, using standard fast-slow coincidence techniques, with respect to the α-particle time signals. Because of the width of the time window used, ~ 20 μs, the relative intensities of the 511-keV line observed in the singles and coincidence data were compared to determine the real to random coincidence rate. From this comparison it was determined that the real to random coincidence rate was 7 to 1.

A γ-γ coincidence experiment with three germanium detectors was carried out at a beam energy of 67 MeV. The three germanium detectors were positioned 5 cm from the target at angles of 90°, −45°, and −120° with respect to the beam direction. In this experiment coincidences between any pair of detectors were accepted and recorded in event mode on magnetic tape for subsequent analysis. The target used for this measurement was a thick, ~ 20 mg/cm^2, ^{209}Bi foil. The beam was stopped a meter downstream of the target position in a shielded Faraday cup. A total of 108 million coincidence events was collected. The replay of these data involved sorting

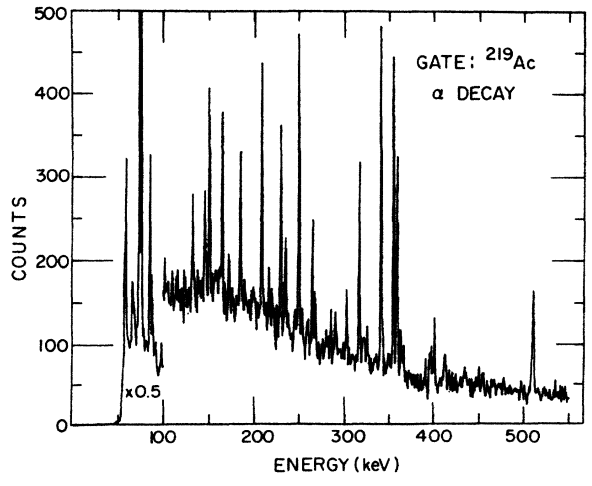

FIG. 3. Gamma rays observed in delayed coincidence with the 9.36 MeV α particle originating from the ground-state decay of ^{219}Ac.

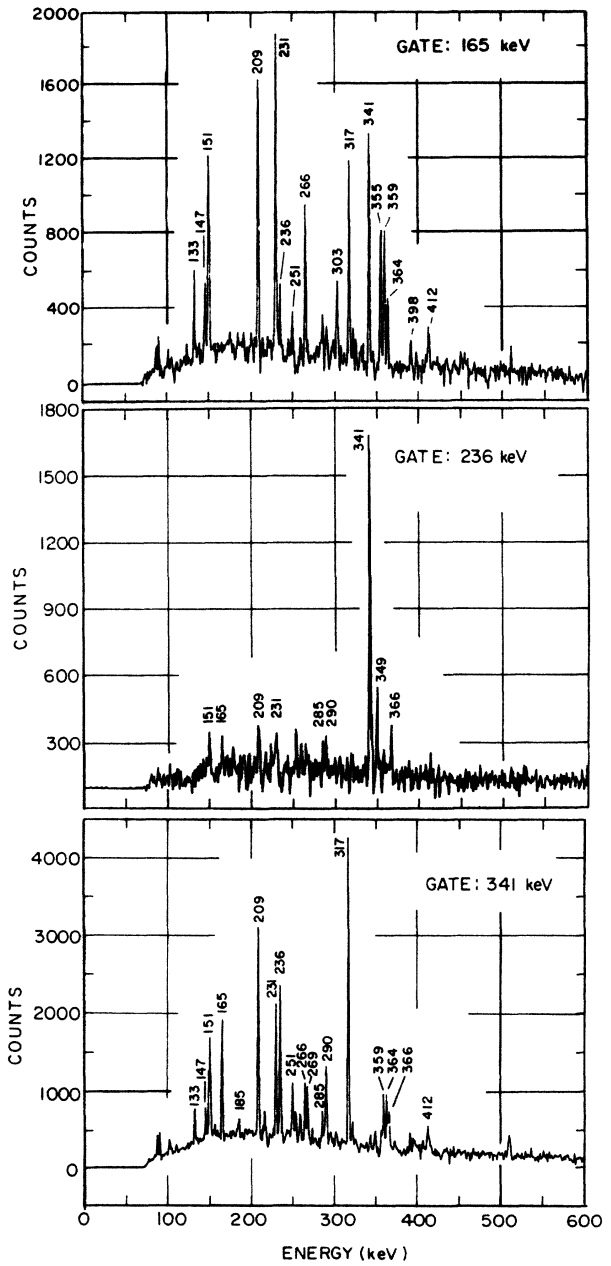

FIG. 4. Compton-subtracted γ-γ coincidence spectra obtained when gating on the 165-, 236-, and 341-keV transitions in ^{219}Ac.

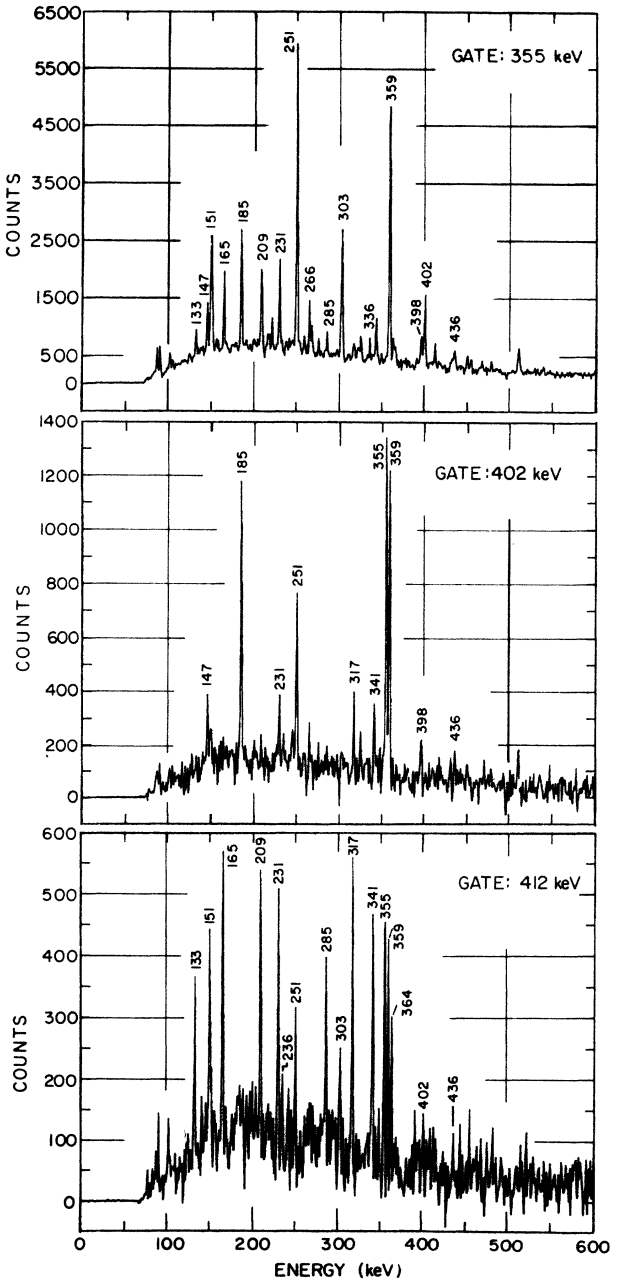

FIG. 5. Compton subtracted γ-γ coincidence spectra obtained when gating on the 355-, 402-, and 412-keV transitions in ^{219}Ac.

each event after correcting the differences in energy calibration of the three germanium detectors by converting the channel numbers into their corresponding energies and binning the results in 0.5 keV steps. Figures 4 and 5 present spectra extracted from selected energy gates after the Compton and random coincidences have been subtracted.

Multipolarity assignments were made from angular distribution data taken at angles ranging from 0° to 90° (with respect to the beam direction) in 15° increments at a ^{13}C beam energy of 67 MeV on the same ^{209}Bi target as described above. Because of the high density of lines present in the singles spectra, three different sets of angular distribution data were collected and analyzed separately and compared to check for consistency. The final results of the angular distribution measurements are presented in Table I. Table II contains the γ-ray intensities, corrected for detector efficiencies, and the proposed J^{π} values for the levels connected by these transitions.

From the angular distribution data a determination of the transition multipolarity was made. This analysis, however, cannot distinguish between electric and magnetic transitions, which is especially important for dipole transitions. To extract this information a linear polarization experiment was performed utilizing the dependence[26] of the Compton scattering cross section on the scattering angle with respect to the direction of the electric field vector E. The apparatus used in this measurement was a three germanium Compton polarimeter similar to those described in the literature.[27–29] Although asymmetries were obtained[13] for some of the transitions in ^{219}Ac, statistics for these low-energy ($E_{\gamma} < 350$ keV) transitions were poor, and definitive assignments of electric versus magnetic nature of these transitions could not be made.

Because of the inconclusive results of the linear polarization measurement, tentative parity assignments to levels have been made on the basis of intensity balancing arguments, taking into account the relative magnitudes of internal conversion coefficients (ICC's) for $M1$ and $E1$ transitions in the high-Z region. For example,[30] for Ac with $Z=89$ the $E1$ K-shell ICC for a 135-keV γ ray is 0.19, whereas for an $M1$ K shell the ICC is 6.14. When the ICC's are taken into account to determine the total transition strengths, we find that in order for the intensities to balance in the level scheme the interband transitions must be $E1$ in character. The quadrupole transitions are electric in character because of their prompt nature.

III. LEVEL SCHEME

In Fig. 6 we present the level scheme for ^{219}Ac as determined from this study. The ground-state spin and parity of $\frac{9}{2}^-$ was proposed in Ref. 25 and the validity of this assignment is supported by the α-particle spectrum. Alpha decay of the ^{219}Ac ground state is observed to the known[25] $\frac{9}{2}^-$ ground state of ^{215}Fr. In the α-particle spectrum (Fig. 2) the ^{219}Ac and ^{215}Fr α-particle peaks are of equal intensity, as expected if all of the ^{219}Ac nuclei are decaying to ^{215}Fr which is then decaying to ^{211}At with the same angular distribution (that is, same angular momentum transfer, $\Delta l = 0$).

The ground state is populated by two parallel cascades. Each cascade consists of a positive- and negative-parity band, in which states in each band are connected by stretched $E2$ transitions with (most probably) $E1$ interband transitions between positive- and negative-parity states in each cascade. The intraband $E2$ transitions are considerably weaker in intensity than the strong stretched dipole transitions and, in the case of those connecting the states within the negative-parity bands, the intensities are

TABLE I. Angular distribution results.

E_γ (keV)[a]	A_2/A_0	A_4/A_0	δ
133.39	−0.34±0.07	0.02±0.09	
146.90	−0.07±0.07	−0.17±0.09	
150.84	−0.10±0.06	−0.12±0.09	
165.24	−0.19±0.07	−0.09±0.07	
185.05	−0.19±0.07	−0.05±0.07	
208.98	−0.18±0.06	−0.09±0.07	
230.65	−0.23±0.07	0.10±0.10	
235.89	−0.15±0.07	−0.03±0.07	
250.70	−0.22±0.06	0.01±0.06	
265.93	−0.13±0.07	−0.02±0.07	
268.95			
285.28	−0.34±0.08	0.04±0.10	
302.49	0.43±0.06	0.06±0.07	
316.61	0.28±0.05	−0.18±0.06	
325.38			
335.67	0.36±0.06	−0.16±0.17	
341.01	0.10±0.05	0.06±0.06	0.25±0.05
349.48	0.13±0.07	−0.11±0.09	
355.19	0.25±0.05	−0.07±0.06	
359.21	0.24±0.06	−0.12±0.09	
360.0±0.3			
363.99	0.27±0.06	−0.10±0.07	
366.44	0.40±0.06	−0.23±0.09	
396.0±0.3			
397.61	0.18±0.07	−0.05±0.09	
401.54	0.21±0.06	−0.06±0.07	
412.27	0.22±0.09	−0.03±0.11	
436.30	0.38±0.41	0.01±0.90	
450.1±0.2	0.38±0.12	−0.25±0.15	
535.01	−0.09±0.06	0.02±0.09	
668.0±0.3			

[a]Uncertainties in quoted energies are ±0.15 keV unless otherwise indicated.

too low to extract statistically significant angular distributions. The highest spin states observed are the $J^\pi = \frac{31}{2}^{(-)}$ state at 2245 keV and the $J^\pi = \frac{31}{2}^{(+)}$ state at 2149 keV. The construction of a level scheme was further complicated by the presence of four transitions (at 147, 151, 251, and 317 keV) which have been multiply placed based on coincidence results. The 251-keV doublet has been particularly troublesome because both transitions have been assigned to the same cascade. Although the parities assigned for the states above the $\frac{15}{2}^-$ and the $\frac{17}{2}^-$ states are tentative because of the uncertainties of the exact natures of the interband transitions, as discussed above, intensity balance requirements would only allow electric dipole transitions. Therefore, in the subsequent discussion we shall assume definite parity assignments.

In addition to the four bands contained in the two main cascades there is a fifth sideband which appears to have a different structure. This band has a $\frac{13}{2}^{(+)}$ bandhead at 577 keV and may be a rotational band built on the $\pi i_{13/2}$ single proton state. A stronger test of this hypothesis will have to wait until more information can be obtained on the natures of the 535- and 668-keV transitions placed in this band so that spin and parity assignments can be made. The available data on this band indicate that the first two transitions are $E2$ in character. The intensities of the 535- and 668-keV transitions are too

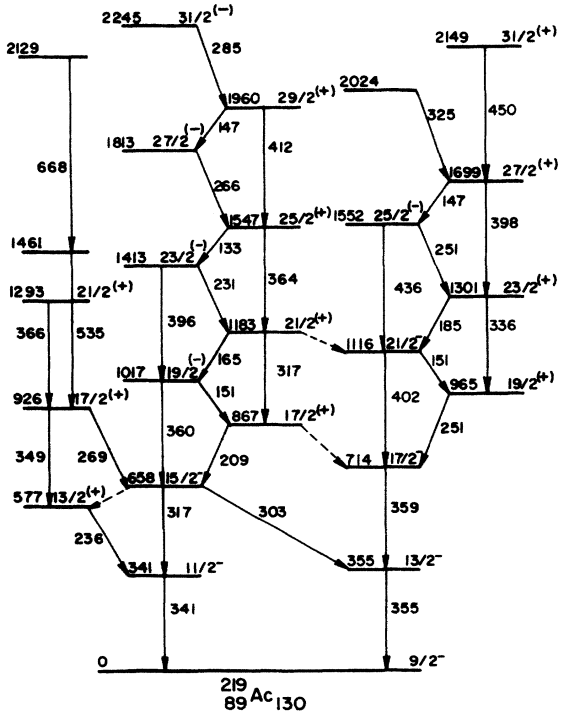

FIG. 6. The level scheme of ^{219}Ac obtained from the ^{209}Bi(^{13}C,3nγ) reaction.

TABLE II. Gamma-ray transitions in ^{219}Ac.

E_γ (keV)	$J_i^\pi \rightarrow J_f^\pi$	I_γ	Character
133.39	$\frac{25}{2}^{(+)} \rightarrow \frac{23}{2}^{(-)}$	15±1	($E1$)
146.90	$\frac{29}{2}^{(+)} \rightarrow \frac{27}{2}^{(-)}$; $\frac{27}{2}^{(+)} \rightarrow \frac{25}{2}^{(-)}$	17±1	($E1$)
150.84	$\frac{21}{2}^{-} \rightarrow \frac{19}{2}^{(+)}$; $\frac{19}{2}^{(-)} \rightarrow \frac{17}{2}^{(+)}$	41±2	($E1$)
165.24	$\frac{21}{2}^{(+)} \rightarrow \frac{19}{2}^{(-)}$	34±2	($E1$)
185.05	$\frac{23}{2}^{(+)} \rightarrow \frac{21}{2}^{-}$	24±1	($E1$)
208.98	$\frac{17}{2}^{(+)} \rightarrow \frac{15}{2}^{-}$	40±2	($E1$)
230.65	$\frac{23}{2}^{(-)} \rightarrow \frac{21}{2}^{(+)}$	29±1	($E1$)
235.89	$\frac{13}{2}^{(+)} \rightarrow \frac{11}{2}^{-}$	20±1	($E1$)
250.70	$\frac{25}{2}^{(-)} \rightarrow \frac{23}{2}^{(+)}$; $\frac{19}{2}^{(+)} \rightarrow \frac{17}{2}^{-}$	52±2	($E1$)
265.93	$\frac{27}{2}^{(-)} \rightarrow \frac{25}{2}^{(+)}$	17±1	($E1$)
268.95	$\frac{17}{2}^{(+)} \rightarrow \frac{15}{2}^{-}$	7±2	isotropic
285.28	$\frac{31}{2}^{(-)} \rightarrow \frac{29}{2}^{(+)}$	4.8±0.3	($E1$)
302.49	$\frac{15}{2}^{-} \rightarrow \frac{13}{2}^{-}$	32±1	($E2$)
316.61	$\frac{15}{2}^{-} \rightarrow \frac{11}{2}^{-}$; $\frac{21}{2}^{(+)} \rightarrow \frac{17}{2}^{(+)}$	50±1	$E2$
325.38	2024 $\rightarrow \frac{27}{2}^{(+)}$		
335.67	$\frac{23}{2}^{(+)} \rightarrow \frac{19}{2}^{(+)}$	3.8±0.3	$E2$
341.01	$\frac{11}{2}^{-} \rightarrow \frac{9}{2}^{-}$	82±4	$M1+E2$
349.48	$\frac{17}{2}^{(+)} \rightarrow \frac{13}{2}^{(+)}$	11±1	$E2$
355.19	$\frac{13}{2}^{-} \rightarrow \frac{9}{2}^{-}$	100±4	$E2$
359.21	$\frac{17}{2}^{-} \rightarrow \frac{13}{2}^{-}$	78±4	$E2$
360.0±0.3	$\frac{19}{2}^{(-)} \rightarrow \frac{15}{2}^{-}$		($E2$)
363.99	$\frac{25}{2}^{(+)} \rightarrow \frac{21}{2}^{(+)}$	14±1	$E2$
366.44	$\frac{21}{2}^{(+)} \rightarrow \frac{17}{2}^{(+)}$	11±1	$E2$
396.0±0.3	$\frac{23}{2}^{(-)} \rightarrow \frac{19}{2}^{(-)}$		($E2$)
397.61	$\frac{27}{2}^{(+)} \rightarrow \frac{23}{2}^{(+)}$	20±1	$E2$
401.54	$\frac{21}{2}^{-} \rightarrow \frac{17}{2}^{-}$	17±1	$E2$
412.27	$\frac{29}{2}^{(+)} \rightarrow \frac{25}{2}^{(+)}$	11±1	$E2$
436.30	$\frac{25}{2}^{(-)} \rightarrow \frac{21}{2}^{-}$	2±1	$E2$
450.1±0.2	$\frac{31}{2}^{(+)} \rightarrow \frac{27}{2}^{(+)}$	3.5±0.2	$E2$
535.01	1461 $\rightarrow \frac{17}{2}^{(+)}$	18±1	isotropic
668.0±0.3	2129 $\rightarrow$ 1461		

weak to permit extraction of their angular distribution coefficients.

Preliminary results of a concurrent study of ^{219}Ac by Khazrouni *et al.*[15] have recently been reported. The level scheme obtained in that study is essentially identical to that presented in this work. The major difference between the two schemes is in the placement of the 577-keV $\frac{13}{2}^{+}$ state which they have assigned to the positive-parity band deexciting through the $\frac{17}{2}^{(+)}$ level at 867 keV. We, however, have placed this transition as the bandhead of the positive-parity sideband. In order to check the validity of our placement of this level in light of this concurrent study, we reexamined our coincidence data for the 290.0-keV transition which Khazrouni *et al.*[15] have placed connecting the $\frac{17}{2}^{(+)}$ and the $\frac{13}{2}^{(+)}$ states. A γ-ray transition of that energy is observed in the γ-γ coincidence spectrum obtained when gating on the 236-keV $\frac{13}{2}^{+}$ to $\frac{11}{2}^{-}$ transition, but there is no evidence for such a γ ray in the coin-

cidence spectrum obtained when gating on the 317-keV $\frac{21}{2}^{(+)}$ to $\frac{17}{2}^{(+)}$ transition. The absence of a 290-keV γ ray in the 317-keV gate is a strong argument against the placement of the $\frac{13}{2}^{(+)}$ state in the same band as the 867-keV $\frac{17}{2}^{(+)}$ state. There is clear support, however, for our placement of the $\frac{13}{2}^{(+)}$ state in that the 341-, 349-, and 366-keV transitions are prominent in the γ-γ coincidence spectrum gated on the 236-keV transition. The other difference in our level scheme from that presented by Khazrouni *et al.*[15] is the total absence of the positive-parity sideband which we have built on the $\frac{13}{2}^{(+)}$ 577-keV state.

IV. DISCUSSION

The original motivation for this study had been to investigate the change in structure from that of single particle excitations, well described by the spherical shell model in the nuclei immediately adjacent to the doubly-magic nucleus ^{208}Pb (Refs. 1, 2, and 31), to the prolate collective rotational structures, well known in the heavier actinides. Since the inception of this study, however, new and exciting questions about the underlying nuclear structure of the nuclei in this mass region have arisen.

Before examining in depth how the predictions of the various models being explored for nuclei in this mass region compare with the structure of ^{219}Ac, it would be pertinent to examine the structural systematics of the light ($A < 225$) Ac isotopes and the $N = 130$ isotones.

Figure 7 presents the systematics of the light Ac isotopes ($215 \leq A \leq 223$). The nuclei ^{215}Ac and ^{217}Ac have level schemes which can be well explained within the context of a spherical shell model.[31,32] For ^{223}Ac, however, the structure has already changed to that of collective rotation observed in the heavier actinides.[25] The level scheme of ^{219}Ac is neither shell-model-like nor collective rotational in nature. In fact, the level spacings are reminiscent of vibrational excitations. From the systematics ^{219}Ac appears to be in the transitional region separating nuclei dominated by single-particle excitations and those dominated by deformed collective excitations.

In Fig. 8 we present the level scheme systematics for the $N = 130$ isotones ^{218}Ra (Refs. 8 and 33) and ^{220}Th (Ref. 16). First we emphasize the similarities in the J^{π} sequences and level energies for ^{218}Ra and ^{220}Th. Comparing these two level schemes with that obtained here for ^{219}Ac, it appears that the energy levels and J^{π} values in ^{219}Ac may be explained in terms of the weak coupling of a $\pi h_{9/2}$ particle to the ^{218}Ra even-even core. There is an additional structural similarity between these nuclei in that strongly enhanced $E1$ transitions have been observed in all three level schemes.[8,16,33]

The positive- and negative-parity states in the two main cascades in ^{219}Ac are connected by strong $E1$ transitions. Reduced relative transition probabilities in Weisskopf units, $B_W(E\lambda)$, were calculated from the extracted intensities. In Table III we present $B_W(E1)/B_W(E2)$ ratios for those levels for which $E2$ angular distributions had sufficient statistics for intensities to be extracted. The

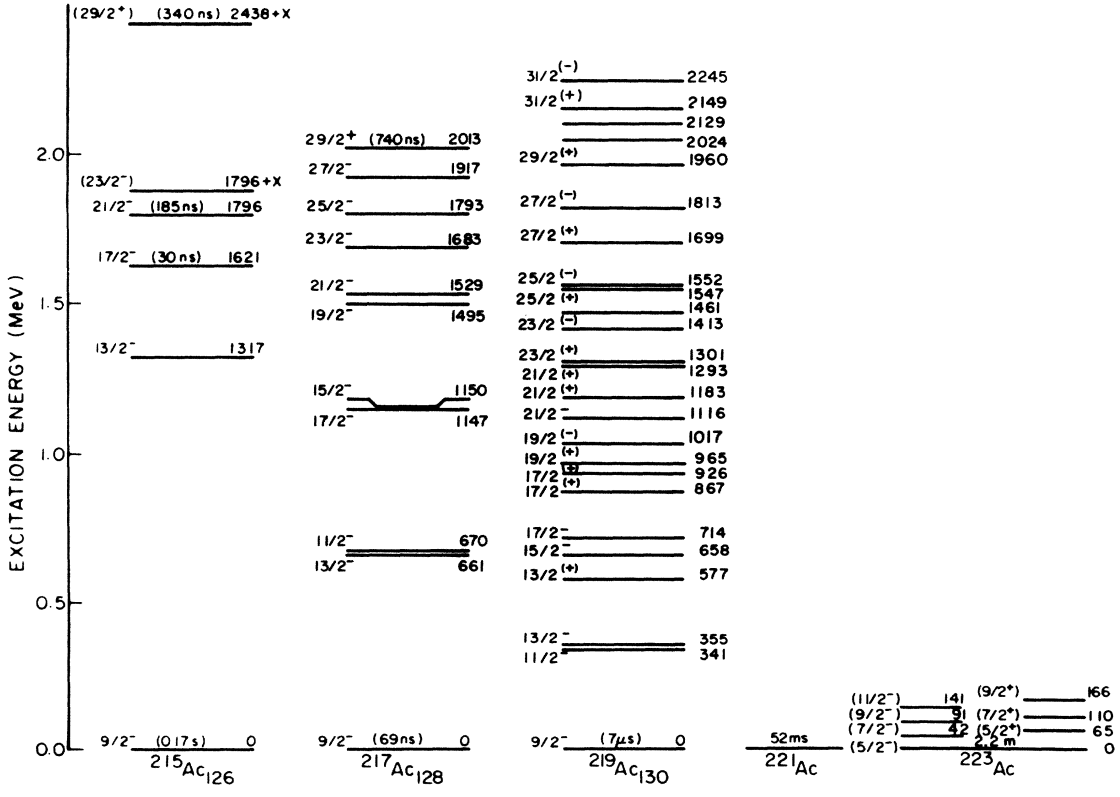

FIG. 7. A comparison of the systematics of the light Ac isotopes ($A < 225$): ^{215}Ac (Ref. 31), ^{217}Ac (Ref. 10), and ^{221,223}Ac (Ref. 19).

TABLE III. $B_W(E1)/B_W(E2)$ ratios in ^{219}Ac.

$\frac{B_W(E1)}{B_W(E2)}$	J^π_{initial}	E_i (keV)
$(1.1\pm0.2)\times10^{-4}$	$\frac{21}{2}^-$	1116
$(1.1\pm0.1)\times10^{-4}$	$\frac{23}{2}^{(+)}$	1301
$(7.2\pm0.5)\times10^{-5}$	$\frac{25}{2}^{(+)}$	1547
$(3.6\pm0.7)\times10^{-5}$	$\frac{27}{2}^{(+)}$	1699
$(6.5\pm1.5)\times10^{-5}$	$\frac{29}{2}^{(+)}$	1960

size of the $B_W(E1)/B_W(E2)$ values obtained indicates relatively strong $E1$ transitions. The range of ratios found in this study extend over the same range of values as those extracted for ^{218}Ra (Refs. 8 and 33), $7.0\times10^{-5} \le B_W(E1)/B_W(E2) \le 9.5\times10^{-5}$, and ^{220}Th (Ref. 16), $8.0\times10^{-5} \le B_W(E1)/B_W(E2) \le 1.0\times10^{-4}$. If we assume that the structure of ^{219}Ac is related to that of ^{218}Ra and take the reported $B_W(E2)$ values[33] for ^{218}Ra of $\simeq$30 W.u. as an estimate of the $B_W(E2)$ strength in ^{219}Ac, we get a $B(E1)\sim0.3\times10^{-2}$ W.u., which constitutes a large $E1$ enhancement.

The similarities of the tabulated $B_W(E1)/B_W(E2)$ ratios is another piece of evidence which together with the similarities in the level spacings support the conclusion that the structures of ^{218}Ra and ^{219}Ac are closely related. This evidence indicates that the level structure of ^{219}Ac could be explainable in terms of a weak coupling of the odd $h_{9/2}$ proton to the ^{218}Ra even-even core.

One of the most interesting aspects of the ^{219}Ac level scheme is the appearance of parity doublets beginning with the $J=\frac{17}{2}$ pair of levels at 714 and 867 keV and proceeding to the top of the observed level scheme to the $J=\frac{31}{2}$ level pair at 2149 and 2245 keV. Parity doublets, especially in the heavier actinides, have been viewed as a necessary, but not conclusive, evidence for the presence of a stable octupole deformation in these nuclei.[21]

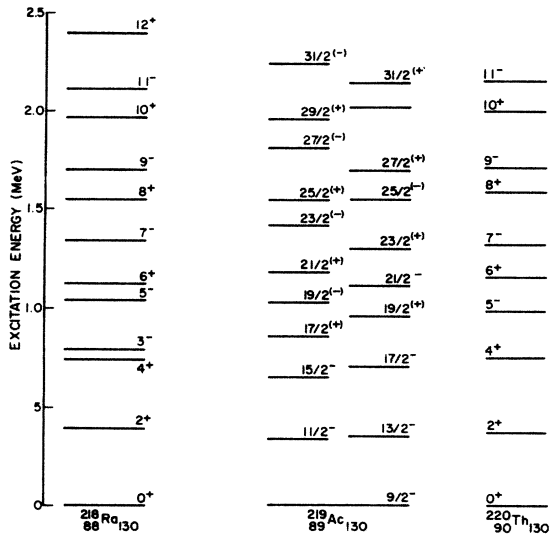

FIG. 8. A comparison of the systematics of the $N=130$ isotones ^{218}Ra (Refs. 8 and 33), ^{219}Ac, and ^{220}Th (Ref. 16).

For the last few years many authors have been using the symmetry under $\hat{R}_x$ of an axial rotor and the associated "signature" quantum number, r. This quantum number cannot be used for systems for which the intrinsic reflection symmetry has been broken. Nazarewicz *et al.*[20] have proposed the use of the symmetry under $\hat{S}=\hat{\pi}\hat{R}_x^{-1}$ (Ref. 34) where $\hat{\pi}$ is the intrinsic parity operator. The quantum number associated with this symmetry is known as simplex, s. The rotating vacuum has a simplex of $s=+1$. The simplex of an excited state can be arrived at by multiplying the vacuum value with the simplex of each quasiparticle.[20] The spin and parity assignment for states in rotational bands described by the different possible simplex values are the following: for $s=+1$

$$J^\pi=0^+,1^-,2^+,3^-,\ldots;$$

for $s=-1$,

$$J^\pi=0^-,1^+,2^-,3^+,\ldots; \quad (1)$$

for $s=+i$,

$$J^\pi=\tfrac{1}{2}^+,\tfrac{3}{2}^-,\tfrac{5}{2}^+,\tfrac{7}{2}^-,\ldots;$$

for $s=-i$,

$$J^\pi=\tfrac{1}{2}^-,\tfrac{3}{2}^+,\tfrac{5}{2}^-,\tfrac{7}{2}^+,\ldots.$$

Using this classification scheme we can label the four main bands in terms of simplex and parity (s,π). The band built on the 341-keV $\frac{11}{2}^-$ level has quantum numbers $(s,\pi)=(i,-)$, the 867-keV $\frac{17}{2}^+$ level is an $(s,\pi)=(i,+)$ state, the $\frac{9}{2}^-$ ground state has $(s,\pi)=(-i,-)$.

The energy splittings of the parity doublets in ^{219}Ac are presented in Table IV. These data have been displayed to show the differences in the energy splittings between the two types of parity doublets as designated by simplex and parity quantum numbers (s,π). The trends exhibited in the energy splittings are different for these two types. The $(i,+)$ and $(-i,-)$ parity doublets start with the positive-parity member of the pair higher in energy than

TABLE IV. Energy splittings of parity doublets labeled with (s,π) values in ^{219}Ac.

J	$E_J(i,+)-E_J(-i,-)$ (keV)	$E_J(-i,+)-E_J(i,-)$ (keV)
$\frac{17}{2}$	153	
$\frac{19}{2}$		−67
$\frac{21}{2}$	67	
$\frac{23}{2}$		−113
$\frac{25}{2}$	−5	
$\frac{27}{2}$		−114
$\frac{31}{2}$		−98

the negative-parity member. Progressing up the level scheme to higher spin, the energy splitting decreases until at the $J=\frac{25}{2}$ pair the negative-parity level becomes higher in energy than the positive-parity level. If the 2024-keV level is confirmed to be a $J^{\pi}=\frac{29}{2}^{-}$ state then the trend toward more negative energy splittings continues. This behavior is quite different from that seen for the $(i,-)$ and $(-i,+)$ parity doublets where the splittings are positive, increasing at higher spin and dropping slightly at the highest spin level placed. The systematics of these energy splittings may indicate a difference in the underlying structure of the two sets of parity doublets. The interpretation of the systematics presented will have to wait for more detailed theoretical work with respect to the predictions of the stable octupole model.

In Fig. 9 we show the behavior of the angular momentum along the rotation axis, J_x, and the quasiparticle energies in the rotating frame E' as functions of the rotational frequency, $\hbar\omega$, for the four (s,π) combinations present in this level scheme. The values were extracted in the usual manner[35] using the expressions,

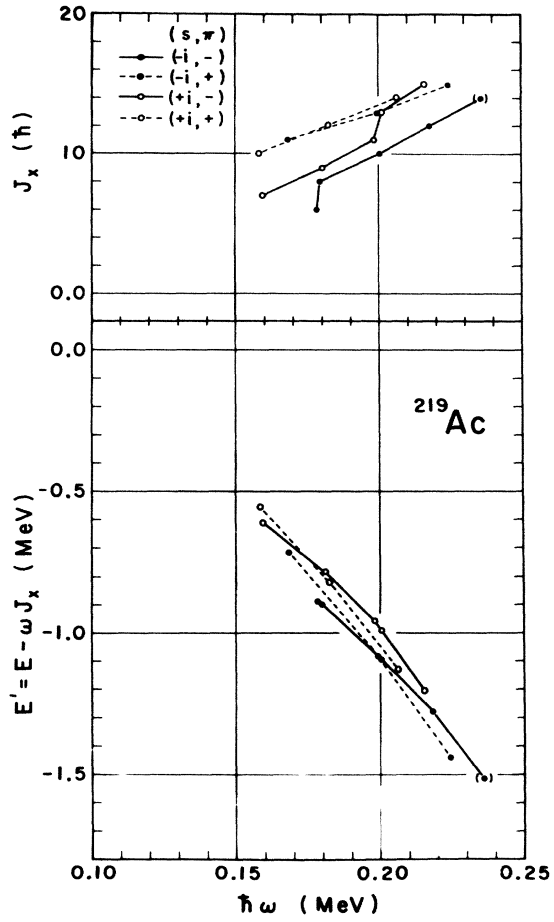

FIG. 9. The levels in ^{219}Ac are plotted in terms of (a) the projections J_x of the angular momentum along the x axis as a function of frequency, and (b) in terms of the quasiparticle energies in the rotating frame as a function of frequency (with no reference taken into account). The levels are labeled in terms of the simplex and parity, (s,π), quantum numbers.

$$\hbar\omega=\frac{E(J+1)-E(J-1)}{J_x(J+1)-J_x(J-1)}\,, \tag{2}$$

$$J_x(J)=[(J+\tfrac{1}{2})^2-K^2]^{1/2}\,, \tag{3}$$

$$E'(J)=E-\omega(J)J_x(J)\,, \tag{4}$$

with a value of $K=0$. No reference configuration was subtracted because of the ambiguities encountered in extracting the reference configurations for the case of ^{222}Th (Ref. 36).

The figure shows that there is considerable simplex splitting between the bands. For both the positive- and negative-parity bands the $s=i$ configuration occurs higher in energy than does the $s=-i$ configuration. The magnitude of the splitting is not the same, however, for the positive- and negative-parity bands. For the negative-parity sequences the energy splitting changes from $\sim$120 keV at $\hbar\omega=0.18$ MeV to $\sim$50 keV at $\hbar\omega=0.215$ MeV. The energy splitting for the positive-parity sequences remains constant at $\sim$60 keV over the entire range observed. For a system with only quadrupole and octupole axial deformations, simplex should be a good quantum number. The presence of considerable simplex splitting may be an indication that additional degrees of freedom, such as triaxiality, may be needed to understand the behavior of ^{219}Ac.

V. CONCLUSIONS

In the present measurement we have obtained the level scheme of ^{219}Ac up to an excitation energy of 2245 keV and angular momentum of $\frac{31}{2}$ from detailed γ-ray spectroscopic measurements. The deexcitation spectrum of ^{219}Ac is characterized by five bands, four of which are based on the proton $h_{9/2}$ configuration, the fifth, most probably, based on the proton $i_{13/2}$ configuration. The four bands have stretched $E2$ intraband transitions; two of these bands are of negative parity, two most probably of positive parity. These bands can be labeled in terms of the simplex and parity quantum numbers, where simplex is the eigenvalue of the operator $\hat{S}=\hat{\pi}\hat{R}_x^{(-1)}$. Even for a nucleus in which the reflection symmetry is broken, the nuclear shape should remain invariant under this operation. The deexcitation pattern is also characterized by stretched, enhanced (most probably) $E1$ transitions between adjacent states with the same simplex value.

The experimentally observed structure of ^{219}Ac presents a new testing ground for the theoretical description of the structure of the light actinides. On the basis of the level spacings and J^{π} values, a weak coupling of the valence proton to ^{218}Ra (Refs. 8 and 33) and ^{220}Th (Ref. 16) core structure is indicated. Additional evidence for this connection is the observation of strongly enhanced $E1$ transitions. From these similarities the nucleus ^{219}Ac provides a testing ground for the future application to an odd-A nucleus of the α-cluster (vibron) model[17] which has been shown to be successful[4,8] in $^{220-226}$Ra and possibly ^{218}Ra. On the other side of the theoretical discussion, the observation of parity doublets, similar to those observed in the heavier and more deformed actinides, can be viewed as an indication of a stable octupole deformation.[18] At this

time the theoretical calculations within this model have not been extended to the more spherical light actinides. While the levels in ^{219}Ac can be labeled in terms of simplex quantum numbers, the considerable simplex splitting observed, and illustrated in Fig. 9, indicates that an additional degree of freedom, in addition to the expected quadrupole and octupole deformations, is needed to explain the structure of ^{219}Ac.

Although the present work presents a detailed level scheme for ^{219}Ac, more experimental measurements are important. The first is a more conclusive determination of the nature of the enhanced interband dipole transitions which at present can only be assumed to be $E1$ in character based on intensity balance arguments. To make this determination, internal conversion electron measurements are being planned. Another important piece of information will result from a measurement of the reduced transition probabilities to determine the absolute strengths of the transitions in ^{219}Ac, since present arguments on the enhancement of $E1$ transitions are only based on $B(E1)/B(E2)$ ratios and preliminary results[33] of absolute $E2$ strengths in ^{218}Ra. It will also be important to extend the level scheme to higher angular momentum, to further study the simplex dependent effects on energy levels observed below $J=\frac{31}{2}$, and to further study what new degree of freedom may be necessary to reproduce these simplex dependent phenomena.

ACKNOWLEDGMENTS

We would like to thank G. Leander and A. J. Larabee for important discussions. This work was supported by the U.S. D.O.E. Contract No. DE-AC02-76ER03074.

*Present address: Physics Department, University of Notre Dame, Notre Dame, IN 46556.

[1]D. Horn, O. Hausser, B. Haas, T. K. Alexander, T. Faestermann, H. R. Andrews, and D. Ward, Nucl. Phys. **A317**, 520 (1979).

[2]T. Lonnroth, D. Horn, C. Baktash, C. J. Lister, and G. R. Young, Phys. Rev. C **27**, 180 (1983).

[3]A. Celler, C. H. Briancon, J. S. Dionisio, A. Lefebvre, C. H. Vieu, J. Zylicz, R. Kulessa, C. Mittag, J. Fernandez-Niello, C. H. Lauterbach, H. Puchta, and F. Riess, Nucl. Phys. **A432**, 421 (1985).

[4]P. D. Cottle, J. F. Shriner, Jr., F. Dellagiacoma, J. F. Ennis, M. Gai, D. A. Bromley, J. W. Olness, E. K. Warburton, L. Hildingsson, M. A. Quader, and D. B. Fossan, Phys. Rev. C **30**, 1768 (1984); J. F. Shriner, P. D. Cottle, J. F. Ennis, M. Gai, D. A. Bromley, J. W. Olness, E. K. Warburton, L. Hildingsson, M. A. Quader, and D. B. Fossan, *ibid.* **32**, 1888 (1985).

[5]J. D. Burrows, P. A. Butler, K. A. Connell, A. N. James, G. D. Jones, A. M. Y. El-Lawindy, T. P. Morrison, J. Simpson, and R. Wadsworth, J. Phys. G **10**, 1449 (1984).

[6]Y. Itoh, Y. Gono, T. Kubo, M. Sugawara, and T. Nomura, Nucl. Phys. **A410**, 156 (1983).

[7]J. Fernandez-Niello, H. Puchta, F. Riess, and W. Trautmann, Nucl. Phys. **A391**, 221 (1982).

[8]M. Gai, J. F. Ennis, M. Ruscev, E. C. Schloemer, B. Shivakumar, S. M. Sterbenz, N. Tsoupas, and D. A. Bromley, Phys. Rev. Lett. **51**, 646 (1983).

[9]N. Schulz, S. Khazrouni, A. Chevallier, J. Chevallier, L. Kraus, I. Linck, D. C. Radford, J. Dudek, and W. Nazarewicz, J. Phys. G **10**, 1201 (1984).

[10]D. J. Decman, H. Grawe, H. Kluge, K. H. Maier, A. Maj, M. Messingen, N. Ray, and W. Wiegner, Nucl. Phys. **A419**, 163 (1984).

[11]M. W. Drigert, J. A. Cizewski, and M. S. Rosenthal, Phys. Rev. C **32**, 136 (1985).

[12]M. W. Drigert and J. A. Cizewski, Bull. Am. Phys. Soc. **29**, 720 (1984).

[13]M. W. Drigert, doctoral dissertation, Yale University, 1984 (unpublished).

[14]M. W. Drigert and J. A. Cizewski, Phys. Rev. C **31**, 1977 (1985).

[15]S. Khazrouni, A. Chevallier, J. Chevallier, O. Helene, G. Ramanantsizehena, and N. Schulz, Z. Phys. A **320**, 535 (1985).

[16]W. Bonin, H. Backe, M. Dahlinger, S. Glienke, D. Habs, E. Hanelt, E. Kankeleit, and B. Schwartz, Z. Phys. A **322**, 59 (1985); W. Bonin, M. Dahlinger, S. Glienke, E. Kankeleit, M. Kramer, D. Habs, B. Schwartz, and H. Backe, *ibid.* **310**, 249 (1983).

[17]F. Iachello and A. D. Jackson, Phys. Rev. Lett. **108B**, 151 (1982).

[18]W. Nazarewicz, P. Olanders, I. Ragnarsson, J. Dudek, G. A. Leander, P. Moller, and E. Ruchowska, Nucl. Phys. **A429**, 269 (1984).

[19]G. A. Leander, R. K. Sheline, P. Moller, P. Olanders, I. Ragnarsson, and A. J. Sierk, Nucl. Phys. **A388**, 452 (1982).

[20]W. Nazarewicz, P. Olanders, I. Ragnarsson, J. Dudek, and G. A. Leander, Phys. Rev. Lett. **52**, 1272 (1984).

[21]G. A. Leander and R. K. Sheline, Nucl. Phys. **A413**, 375 (1984).

[22]K. Nybø, T. F. Thorsteinsen, G. Løvhøiden, E. R. Flynn, J. A. Cizewski, R. K. Sheline, D. Decman, D. G. Burke, G. Sletten, P. Hill, N. Kaffrell, W. Kurcewicz, and G. Nyman, Nucl. Phys. **A408**, 127 (1983).

[23]R. K. Sheline, D. Decman, E. R. Flynn, J. A. Cizewski, D. G. Burke, G. Sletten, P. Hill, N. Kaffrell, W. Kurcewicz, G. Nyman, and G. Leander, Phys. Lett. **133B**, 13 (1983).

[24]R. R. Chasman, Phys. Lett. **96B**, 7 (1980).

[25]*Table of Isotopes*, 7th ed., edited by C. M. Lederer and V. S. Shirley (Wiley, New York, 1978).

[26]D. Pelte and D. Schwalm, *In Beam Gamma-ray Spectroscopy with Heavy Ions, Heavy Ion Collisions*, edited by R. Bock (North-Holland, Amsterdam, 1982), Vol. 3.

[27]A. Poletti, Phys. Rev. **153**, 1108 (1967).

[28]K. Ashibe, M. Adachi, and H. Taketani, Nucl. Instrum. Methods **130**, 221 (1975).

[29]J. Kosagi, N. Kishido, and H. Ohnumo, Nucl. Instrum. Methods **144**, 201 (1977).

[30]R. S. Hager, and E. C. Seltzer, At. Data Nucl. Data Tables **1**, 1 (1973).

[31]D. J. Decman, H. Grawe, H. Kluge, and K. H. Maier, Z. Phys. A **310**, 55 (1983).

[32]D. J. Decman, H. Grawe, H. Kluge, K. H. Maier, A. Maj, N.

Roy, Y. K. Agarwal, K. P. Blume, M. Guttormsen, H. Hubel, and J. Recht, Nucl. Phys. **A436**, 331 (1985).
[33]J. F. Ennis, doctoral dissertation, Yale University, 1984 (unpublished).
[34]A. L. Goodman, Nucl. Phys. **A230**, 139 (1980).
[35]R. Bengtsson and S. Frauendorf, Nucl. Phys. **A327**, 139 (1979).
[36]D. Ward, G. D. Dracoulis, J. R. Leigh, R. J. Charity, D. J. Hinde, and J. O. Newton, Nucl. Phys. **A406**, 591 (1983).